Volume 14, Issue 1, Page 197-203, 2025 https://doi.org/10.46810/tdfd.1537189 Research Article

BİNGÖL UNIVERSITY

Türk Doğa ve Fen Dergisi
Turkish Journal of Nature and Science

www.dergipark.gov.tr/tdfd

Deterministic Lateral Displacement System with Inclined Elliptical Obstacles for Efficient Size-Based Separation of Microparticles

Döne SAYARCAN[1*], Ahmet CİCEK[2], Nurettin KOROZLU[2]

[1] Opticianry Programme, Gölhisar Vocational School of Health Services, Burdur Mehmet Akif Ersoy University, Burdur, Türkiye
[2] Department of Nanoscience and Nanotechnology, Art and Science Faculty, Burdur Mehmet Akif Ersoy University, Burdur, Türkiye
Döne SAYARCAN ORCID No: 0000-0001-7000-0354
Ahmet CİCEK No: 0000-0002-7686-0045
Nurettin KOROZLU No: 0000-0002-0899-0227

**Corresponding author: donesayarcan@mehmetakif.edu.tr*

(Received: 22.08.2024, Accepted: 07.03.2025, Online Publication: 26.03.2025)

Keywords
Microfluidics, Deterministic lateral displacement (DLD), Particle separation, Finite-element method

Abstract: A deterministic lateral displacement system with inclined elliptical posts is demonstrated to sort spherical micrometer-sized solid particles. Numerical simulations via the finite-element method are performed to investigate the microfluidic system performance. Soft microparticles undergo deformations in designs with cylindrical posts or posts with sharp corners. Such deformations occur due to particle clogging between obstacles, which can disrupt the flow lanes. The proposed approach aims to eliminate these challenges. The calculations reveal a much-reduced rate of change in flow velocity between vertically inclined elliptical posts, compared to circular posts. The calculated critical particle sizes are more likely to follow the equation associated with the first flow lane width derived from a parabolic velocity profile at high fluid inlet rates, rather than the two semi-analytical models proposed for circular posts. The experimental and theoretical critical diameter data exhibited greater agreement with the critical diameter equation obtained using the curve-fitting method at lower fluid inlet rates. Overall, the minimum particle size decreased as the rate of flow increased. When assessing the connection between the two, a smaller critical diameter is achieved by decreasing the inclination angle. The adjustability of the system by rotating the posts is a major advantage of the proposed approach.

Miroparçacıkların Boyutlarına Göre Verimli Ayrıştırılması İçin Eğimli Eliptik Engeller İçeren Bir Deterministik Yanal Yerdeğiştirme Sistemi

Anahtar Kelimeler
Mikroakışkanlar, Deterministik yanal yerdeğiştirme (DYY), Parçacık ayrıştırma, Sonlu elemanlar yöntemi

Öz: Eğik eliptik sütunlar içeren bir Deterministik Yanal Yerdeğiştirme sistemi, mikrometre boyutundaki küresel katı parçacıkları ayırmak için gösterilmiştir. Mikroakışkan sistem performansını araştırmak için Sonlu Elemanlar Yöntemi ile sayısal simülasyonlar yapılmıştır. Yumuşak mikroparçacıklar, silindirik sütunlar veya keskin köşelere sahip sütunlarla tasarımlarda deformasyonlara uğrar. Bu tür deformasyonlar, parçacıkların engeller arasında tıkanmasından kaynaklanır ve bu da akış yollarını bozabilir. Önerilen yaklaşım, bu zorlukları ortadan kaldırmayı hedeflemektedir. Hesaplamalar, dairesel sütunlara kıyasla dikey eğimli eliptik sütunlar arasında akış hızındaki değişim oranının çok daha düşük olduğunu ortaya koymaktadır. Hesaplanan kritik parçacık boyutlarının, yüksek sıvı giriş hızlarında parabolik bir hız profilinden türetilen ilk akış yolu genişliğiyle ilişkili denklemi, dairesel sütunlar için önerilen iki yarı-analitik modelden daha fazla takip etme olasılığı vardır. Deneysel ve teorik kritik çap verileri, daha düşük sıvı giriş hızlarında eğri uydurma yöntemi kullanılarak elde edilen kritik çap denklemi ile daha büyük bir uyum sergilemiştir. Genel olarak, minimum parçacık boyutu akış hızı arttıkça azalmıştır. İkisi arasındaki bağlantı değerlendirildiğinde, eğim açısının azaltılmasıyla daha küçük bir kritik çap elde edilir. Sütunları döndürerek sistemi ayarlayabilme imkanı, önerilen yaklaşımın büyük bir avantajıdır.

1. INTRODUCTION

Microfluidic devices for particle sorting in suspensions have attracted attention in the fields of biomedical research, biochemistry, pharmacology, and clinical diagnostics [1, 2]. Typically, such sorting procedures can be carried out via centrifugation, flow cytometry, gel electrophoresis, and chromatography. Although these techniques are effective for samples with a high volume, they are not suitable for small-scale operations. Microfluidic systems provide the reduction in size and combination of different functionalities to carry out laboratory tasks on a small scale. These systems can handle, combine, and examine small amounts of samples, while significantly reducing the amount of time needed to conduct such operations.

Microfluidic systems have extensive applications in the manipulation, sorting, and classification of micro- and nanoparticles [3]. Particle manipulation is frequently employed in the detection of biomolecules [4], as well as in the sorting and separation of cells [5, 6]. Particle sorting strategies in microfluidics can be categorized into active and passive schemes. Active sorting devices including magnetophoresis [7], dielectrophoresis [8], acoustophoresis [9], and thermophoresis [10] control the movement of particles by applying external forces. These approaches depend on the interaction between the particles and either the flow, magnetic, electric, acoustic, or optical field available in the microchannel. Passive microfluidics employs fluid forces and channel geometry to accomplish particle sorting. This involves techniques such as hydrodynamic filtration [11], pinched flow fractionation [12], inertial microfluidics [13], viscoelastic separation [14], and deterministic lateral displacement (DLD) [15]. DLD has gained significant popularity as a technique for particle separation and detection in the last two decades. DLD employs hydrodynamic forces, channel shape, and flow to achieve separation without the need for external forces.

The concept of DLD was first presented by Huang et al. in 2004 [16]. Researchers discovered that in a microchannel, when obstacles are organized in a particular periodic order, laminar flows with Reynolds numbers less than one (Re<1) result in the formation of a specific number of flow lanes (N) between the posts. Microparticles that are smaller than a critical diameter (D_c) have a distinct flow lane, while particles that are larger than Dc follow consecutive flow lanes. These patterns of movement, referred to as zigzag and displacement modes, were described by Huang et al. (2004) [16]. The observed differentiation in the particle trajectories enables the particles to be selectively steered towards specific exit pathways according to their size.
The paths followed by particles passing through a DLD system depend on the geometric parameters of the system. The first of these parameters are: the gap size (G) between two obstacles, the center-to-center distance (λ) between two obstacles, the shift amount ($\Delta\lambda$) of the next obstacle row, and the row shift fraction (ε), which is defined as $\varepsilon = \Delta\lambda/\lambda$. There are various approaches for determining the critical particle size.

Inglis et al. [17] proposed an analytical approach to determine the critical particle diameter (D_c) in a DLD device with equal downstream and lateral gap sizes. The number of flow lanes between obstacles is equal to the period of the obstacle arrays, and the number of flow lanes N is related to the row shift fraction as $N = 1/\varepsilon$ [17]. Each of these flow lanes contains an equal amount of fluid, and the width of each lane can be calculated considering a symmetric parabolic flow profile. According to the theory, if the particle radius is smaller than the width of the first flow lane, the particle follows the lane path, which is termed as the 'zigzag mode' [17]. On the other hand, if the particle radius is larger than the flow lane width, the particle follows successive lanes, termed as the 'displacement mode'. The width β of the "first" flow lane passing through each row gap (adjacent to the row) is given as a first-order approximation by

$$D_c = 2\beta \tag{1}$$

Considering a parabolic velocity profile between adjacent obstacles and the equal flux carried by the flow lanes, β can be analytically calculated [17]. Beech [19] simplified the critical particle diameter equation to

$$\frac{D_c}{G} = 1.155\varepsilon^{0.5} \tag{2}$$

Davis [18] derived an empirical formula for the critical particle size in a DLD device:

$$D_c = 1.4G\varepsilon^{0.48} \tag{3}$$

Equation (3) according to Davis' [18] theory is obtained by investigating approximately 20 different devices in experiments, in which polystyrene beads were used to collect data [15]. Non-spherical and deformable particles were not considered in Davis' [18] study.

Conducting a theoretical analysis of DLD devices improves the accuracy of predicting the paths of particles. Many DLD systems with varying obstacle configurations have been investigated to the date. Analyses have been conducted on systems that feature posts with different shapes, including airfoil-shaped [20], teardrop-shaped [21], triangular [22], I-shaped [23], and optimized-shaped [24]. Asymmetric systems, characterized by unequal lateral and downstream gaps, have also been studied to determine the critical particle diameter. Inglis et al. [17] introduced a theoretical method to calculate the critical particle size in asymmetric DLD designs. Zhang et al. [13] conducted a numerical analysis to investigate the impact of several column forms (cylindrical, diamond, and triangular) on the dynamic behavior of red blood cells in DLD devices. Sharp and pointed obstacles drastically increase the probability of red blood cells to deform and result in considerable damage.

As previously stated, numerous DLD systems have been developed by leveraging the characteristics of the particles that need to be sorted. The efficiency of the proposed DLD systems is significantly influenced by

various characteristics, including the geometric parameters of the DLD system, the shapes of obstacles, the properties of the fluid, and the properties of the particles. Due to the numerous parameters that affect the system, additional research and the development of more DLD systems are required.

This research focuses on a DLD system including inclined elliptical posts, a design that has not been previously investigated. First, the performance of the proposed device is assessed. After that, an analysis is conducted on the efficacy of particle sorting, the impact of fluid velocity on particle paths, and the influence of obstacle inclination angles. The separation capability of the designed system is assessed by comparing the calculated critical diameters with those predicted through the formulas presented by Inglis [17] and Davis [18] for DLD systems that have circular obstacle posts. The velocity profile between the elliptical obstacle posts is compared to the profile in a conventional design, taking into account the impact of the velocity profile on the sorting of particles. The effect of the inclination angle of the elliptical obstacle posts on the critical diameter has been examined. The system under consideration has been modeled through two-dimensional (2D) finite element method (FEM) simulations. A module for particle tracking, which includes an interface for fluid-particle interaction, was used to simulate the interactions between the particles and the obstacle posts. This method enabled more accurate prediction of the particle movements. The study employed time-dependent bidirectional particle tracking to determine the threshold particle diameter and track the paths of the particles.

2. MATERIAL AND METHOD

2.1. Simulation Domain Design and Boundary Conditions

To model particle movements in the DLD array, COMSOL Multiphysics software is employed. The model is created using the Particle Tracing for Fluid Flow interface added to the fluid flow module with 2D FEM. The fluid-particle interaction interface is used to account for the effect of particle movement on the fluid flow profile. The microchannel structure was designed using the microfluidic module (Figure 1(a)) and the design parameters of the DLD system (Figure 1(b,c)) are shown in Figure 1.

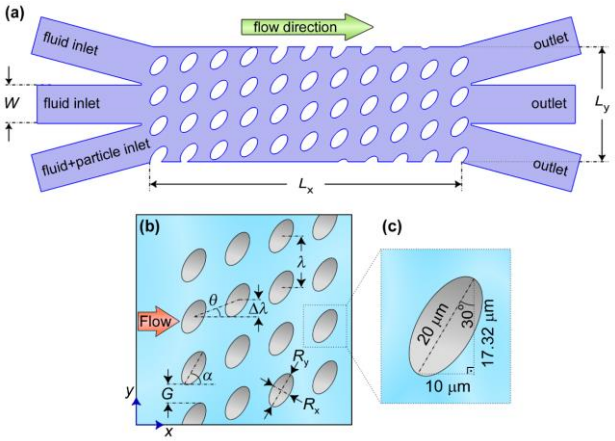

Figure 1: (a) Full-scale depiction of the planned microchannel structure, (b) design of the elliptical DLD posts and the relevant geometrical parameters, (c) geometric position and dimensions of an obstacle post within the DLD system.

The left section of the microfluidic channel is partitioned into three distinct channels for fluid inflow (Figure 1(a)). The right section is further partitioned into three distinct channels for the discharge of fluids and particles (Figure 1(a)). The lowest inlet channel is configured to release particles simultaneously with the stream. The fluid phase utilized water at ambient temperature. The input flow is characterized by a parabolic velocity profile and a fully developed creeping flow. The outflow boundary condition is specified as having zero viscous stress and Dirichlet conditions on pressure. The fluid in the simulation is subjected to a 'no-slip' condition by the domain walls and fixed obstacle walls. Particles with a density of 1200 kg m³ are specified (Table 1). The drag force, which is influenced by the characteristics of the fluid, operates upon the solid particles. The boundary condition for the particles is specified as 'bounce' when they bumped into the walls. The DLD system is encountered by water and particles immediately after they pass through the entrance channel. The channel width of the DLD system is L_y=99 µm, and its length is L_x=285 µm (Figure 1(a)). The microchannel contains eleven rows of elliptical obstacles, which results in the minimum DLD system length for efficient particle separation. The elliptical obstacle posts are designed with a width of 10 µm and a length of 20 µm to create a fully formed elliptical structure (Figure 1(b)). The minor-to-major axis ratio of the posts is set at ½. The elliptical obstacle posts are placed at a 60° angle relative to the direction of flow (the x axis) (Figure 1(c)). G is the gap size between the obstacle posts, λ is the row shift step (same for both x and y directions), and $\Delta\lambda$ is the shift amount between neighboring rows. The row shift fraction is $\varepsilon = \Delta\lambda/\lambda$, and the row shift angle of the obstacle posts is $\theta = \tan^{-1}(\varepsilon)$. Table 1 contains the parameters of the DLD system.

Table 1: Geometrical and physical parameters assumed in the design of the DLD system.

	Parameter	(Unit)	Value	Description
Geometrical	L_x	(μm)	285	Channel length in the propagation (x) direction
	L_y	(μm)	99	Channel height in the lateral (y) direction
	W	(μm)	33	Fluid inlet channel width
	R_x	(μm)	10	Elliptical posts' minor axis length
	R_y	(μm)	20	Elliptical posts' major axis length
	α	(°)	60	Elliptical posts' inclination angle
	G	(μm)	6	The gap between two posts
	$\Delta\lambda$	(μm)	2.25	The row shift
	λ	(μm)	26	Center-to-center distance between posts
	$\varepsilon = \Delta\lambda/\lambda$		0.0865	Row shift fraction
	$\theta = \tan^{-1}(\varepsilon)$	(°)	11.53	Row shift angle
Physical	ρ_f	(kg m^3)	1000	Fluid density
	ρ_p	(kg m^3)	1200	Particle density
	U_f	(μl min-1)	125	Inlet flow rate

To solve the governing equations, it is necessary to create a mesh for the simulation domain. COMSOL utilizes the governing equations to solve for the most precise outcome at every mesh location. A free triangular mesh with a maximum and minimum element size of 4.22×10^{-6} and 6.03×10^{-8}, respectively, is utilized for the calculations. The mesh is specifically designed to comply with the boundary conditions and geometry of the calculation domain. The mesh quality for the present simulation is determined to be 0.8306, implying a high level of mesh quality [25].

Particle motion in a dilute flow is influenced by the fluid. This phenomenon is commonly known as two-way coupling. The Particle Tracing for Fluid Flow interface utilizes the fluid-particle interaction physics to compute the two-way coupling between particles and the fluid. A drag force proportional to the fluid velocity is applied to the particles under laminar flow. The fluid-particle interaction physics solves the Navier-Stokes equations [26, 27] and the continuity equation in a time-dependent manner. The Bidirectionally Coupled Particle Tracing interface, which addresses all particle degrees of freedom in a time-dependent solution, is employed. The remaining degrees of freedom are computed using a stationary solver. A for-end for loop is used to iterate the two solvers and get a self-consistent solution, taking into account the bidirectional interactions between moving particles and the stationary flow field. The time-dependent solver is configured with time steps of 0.001 milliseconds. The 'generalized alpha' method, which is an implicit solver, is used for the time steps. The MUMPS algorithm is the direct solver of choice.

3. RESULTS

This section evaluates the validity of the designed device through numerical calculations and determines the optimal physical conditions for this system.

3.1. Velocity Field

The velocity field between the obstacle gaps significantly affects particle orientation and the deformation of deformable particles. The creeping flow module is used to model the flow behavior within the DLD system. The velocity profiles between traditional circular posts (Figure 2(a)) and the elliptical obstacle posts in this design (Figure 2(b)) are shown in Figure 3. The circular post diameter is chosen to be equal to the sine of the elliptical obstacle diameter given in Figure 2(b) (17.32 μm), and all other DLD parameters are set the same as in this study, with a fluid flow rate of 125 μl min^{-1}.

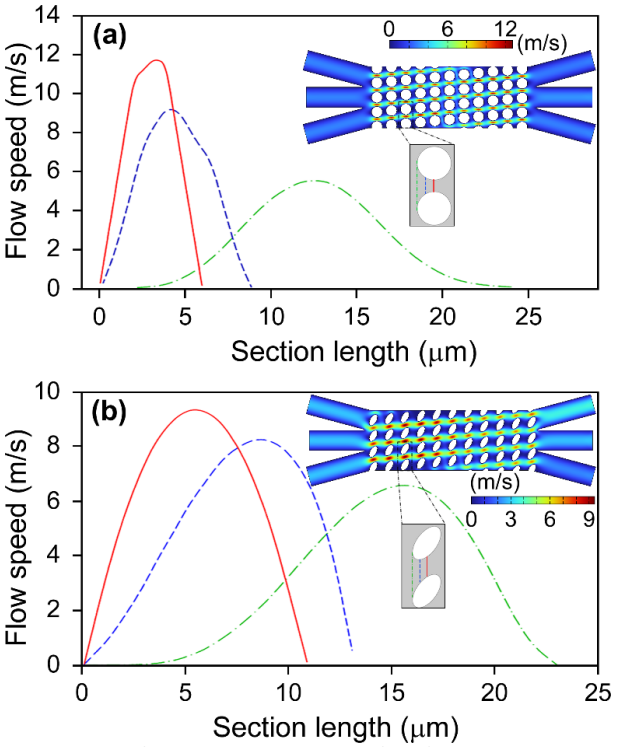

Figure 2: The fluid velocity gradient and flow field between obstacle posts in a DLD system comprised of (a) conventional circular posts and (b) the designed elliptical obstacle posts.

The velocity gradient in the gap between traditional circular post arrays (Figure 2(a)) is relatively higher than the velocity gradient in the gap between elliptical obstacles in the proposed design (Figure 2(b)). The

acceleration in the flow field from the inlet to the closest distance between obstacles (green-blue-red sections, respectively) is almost twice the value calculated for elliptical rods. Besides, the flow speed reaches its maximum values at the closest distance between obstacles (red curve) in both designs. In the traditional design, the flow compresses in the red section, causing the fluid velocity to nearly double compared to the green section (Figure 2(a)). In the proposed design, however, the velocity trend undergoes less variation from the inlet (green section) to the closest distance between obstacles (red section) (Figure 2(b)).The high velocity gradient in the traditional circular post array design has a significant impact on the motion of soft particles, as such particles tend to be rotated, deformed, and subsequently aligned with the average flow direction, leading to no further displacement. In contrast, in our proposed design, the orientation of the elliptical obstacles distributes the velocity gradient over a wider area, creating a more uniform velocity field. Therefore, it can be stated that the elliptical obstacles act as a guide for pressure on transported particles. Additionally, the deformation process of soft particles will be less affected, and the particles will be influenced less by this velocity field.

3.2. Critical Particle Size

For analyzing the impact of changes in $\Delta\lambda$ on critical diameter, simulations of particle trajectories across a range of sizes are conducted. The $\Delta\lambda$ values are systematically increased from 1 µm to 2.75 µm in increments of 0.25 µm. The results are compared with the critical particle sizes obtained from Beech's [28] (Equation 2) and Davis' [18] (Equation 3) formulas (Figure 4). The critical particle size range is determined by finding the smallest diameter of particles in displacement mode and the largest diameter in zigzag mode.

Figure 3 shows the particle movement modes at different ε values and different speeds. Figure 3(a), (b) and (c) shows the particle trajectories at a fluid inlet rate of 100 µl min^{-1}, 125 µl min^{-1}, and 150 µl min^{-1}, respectively, at all inlet channels in Figure 1(a), according to the displacement fraction.

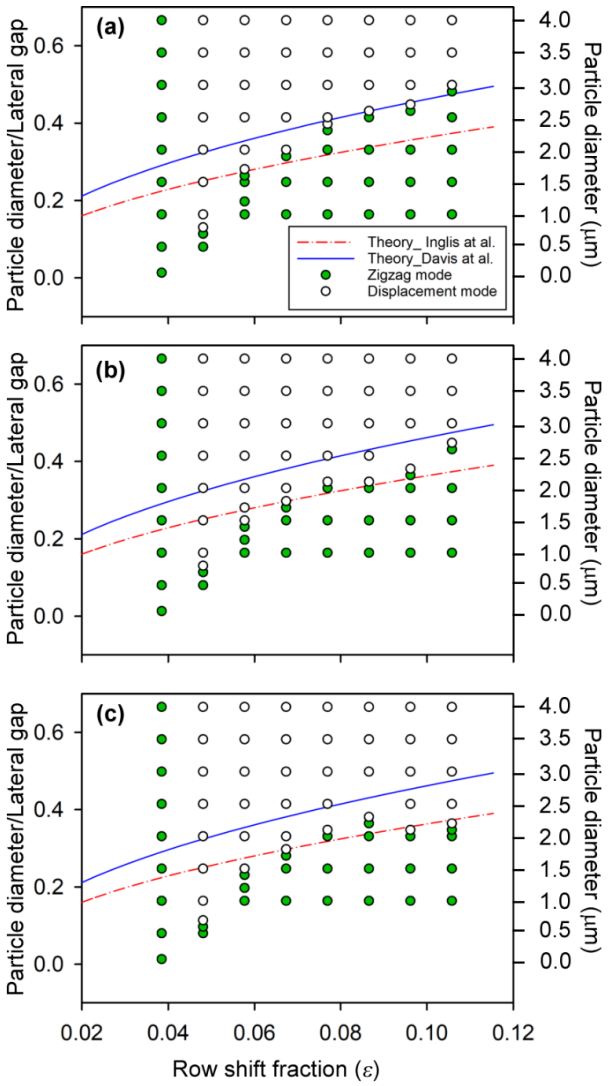

Figure 3: Particle trajectories normalized by obstacle gap size and fluid velocities of **(a)** 100 µl min^{-1}, **(b)** 125 µl min^{-1}, and **(c)** 150 µl min^{-1} based on row shift fraction. The filled and hollow circles represent the zigzag mode and the displacement mode, respectively. Burada The red dashed curve represents the critical diameter curve derived from Inglis et al.'s [17] critical diameter theory, while the blue curve illustrates the critical diameter curve introduced by Davis et al. [18].

The particle size normalized by the lateral obstacle gap size is presented in Figure 3. As the row shift fraction decreases, the hydrodynamic resistance against the switching flow increases, resulting in a very thin first flow lane width (β) for small ε values compared to the direct flow. Since the critical diameter is directly related to the switching flow, the critical diameter decreases as ε decreases. As shown, for $\Delta\lambda$ values of 1 µm and below, particles of all sizes are found to move in zigzag mode, indicating that the obstacle row shift amount should be above 1 µm for the system to operate efficiently. As the row shift fraction increases, the sizes of particles moving in zigzag mode also increase. The critical diameter values for fluid velocities of 125 µl min^{-1} (Figure 3(b)) and 150 µl min^{-1} (Figure 3(c)) are more consistent with the critical diameter model proposed by Inglis et al. [17]. For a fluid velocity of 100 µl min^{-1} (Figure 3(a)), the critical diameter values are more consistent with Davis' [18] proposal.

Besides the row shift fraction, inlet flow rate also affects the critical diameter. The impact of this rate on particle trajectories is shown in Figure 4. A particle with a diameter of 2.5 µm is observed to move in zigzag mode after the eighth obstacle for a rate of 100 µl min^{-1}, while it moves in displacement mode for 125 µl min^{-1} . As the rate increases, the Reynolds number also increases, causing flow lane compression, influencing particle trajectories, and altering separation dynamics [21]. An increase in the Reynolds number generally leads to a decrease in critical diameter, and higher fluid velocities result in denser flow lanes, reducing critical diameter. This result is consistent with the study by Dincau et al [21], which showed that fluid velocity and Reynolds number affect particle trajectories in a DLD system with circular posts.

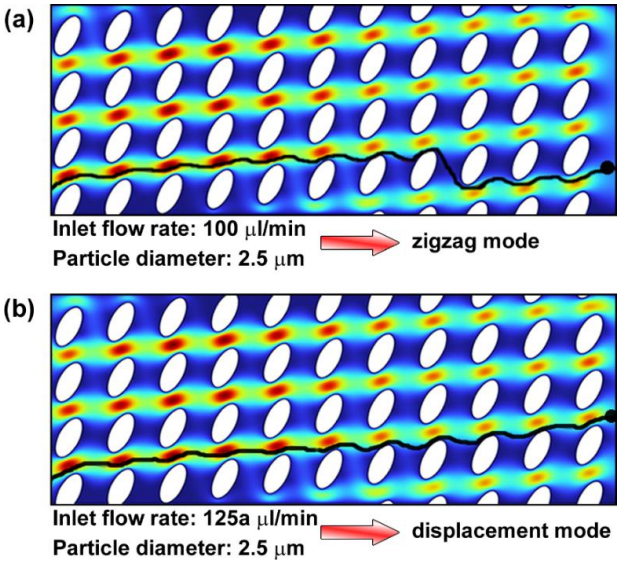

Figure 4: Trajectories of a solid spherical particle with a diameter of 2.5 µm in the DLD system for inlet flow rates of **(a)** 100 µl min^{-1} and **(b)** 125 µl min^{-1}.

The proposed design allows the evaluation of the effect of the inclination angle of elliptical obstacle posts on particle trajectories for an inlet rate of 125 µl min^{-1} and $\Delta\lambda$=2.25 µm. Here, particle trajectories are tracked at various inclination angles. Figure 5 shows particle trajectories based on the inclination angle of the obstacle posts. The selected inclination angle (60°) did not affect the critical diameter within ±5°. When the inclination angle is 70°, the critical particle size decreases, whereas it increases for 50°. Additionally, the critical diameter increases significantly with a decrease in the inclination angle.

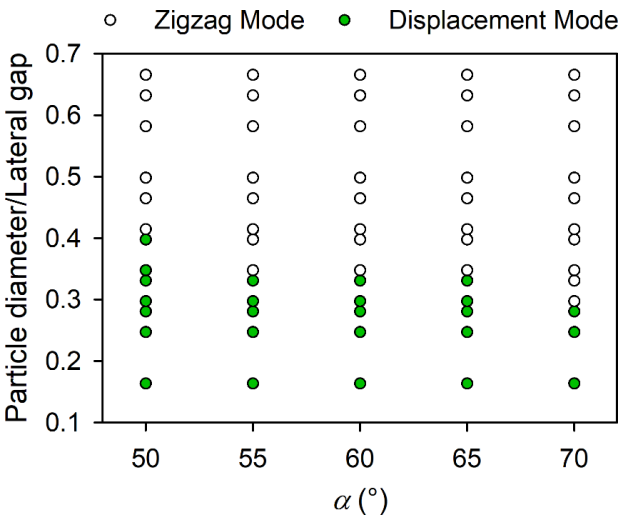

Figure 5: Trajectories of particles of various sizes based on the inclination angle of elliptical obstacle posts.

4. DISCUSSION AND CONCLUSION

In conclusion, an alternative microfluidic device that utilizes the deterministic lateral displacement principle to effectively sort particles within the diameter range of 1 to 4 µm is proposed. The elliptical post design is intended to alleviate the challenges associated with employing conventional circular or sharp-cornered (e.g. triangular, rectangular, etc.) post arrays and presents an original obstacle post design. Hence, adverse effects, such as particle clogging and unintended deformation of soft particles are eliminated through the introduced design.

It is shown that a DLD system including inclined elliptical obstacle posts results in a smoother velocity profile, as the velocity gradient between the circular posts is significantly higher, resulting in a strong tendency for particle rotation, deformation, and alignment with the average flow direction. The use of inclined elliptical posts mitigates these problems by increasing the spacing between the posts, which led to an approximately 50% rise in flow velocity from the input to the midgap between vertically neighboring obstacles. The DLD system displayed behavior that closely aligned with the proposed equation for the initial flow lane width, which was derived from a parabolic velocity profile at high fluid velocities, when compared to the two suggested techniques for circular posts.

The critical diameter equation developed by curve fitting actual and theoretical data showed greater consistency at low inlet flow rates (100 µl min^{-1}). The critical particle diameter reduced as the inlet rate increases. Furthermore, the degree of inclination of the elliptical obstacle posts has an impact on the trajectories of particles since the critical particle diameter is almost constant at inclinations of 55°, 60°, and 65°, but decreases at an inclination of 70° and increases at an inclination of 50°. Thus, the proposed approach is practically adjustable through the rotation of the posts.

Acknowledgement

This work was supported by The Scientific and Technological Research Council of Türkiye (TÜBİTAK) under grant number 117F403 and by The Scientific Research Projects Coordination Unit of Burdur Mehmet Akif Ersoy University under grant number 357YL16.

REFERENCES

[1] Whitesides GM. The origins and the future of microfluidics. Nature. 2006;442(7101):368-73.
[2] Yager P, Edwards T, Fu E, Helton K, Nelson K, Tam MR, Weigl BH. Microfluidic diagnostic technologies for global public health. Nature. 2006;442(7101):412-8.
[3] Salafi T, Zeming KK, Zhang Y. Advancements in microfluidics for nanoparticle separation. Lab on a Chip. 2017;17(1):11-33.
[4] Xu X, Sarder P, Kotagiri N, Achilefu S, Nehorai A. Performance analysis and design of position-encoded microsphere arrays using the Ziv-Zakai bound. IEEE Transactions on Nanobioscience. 2012;12(1):29-40.
[5] Choi J-W, Oh KW, Thomas JH, Heineman WR, Halsall HB, Nevin JH, et al. An integrated microfluidic biochemical detection system for protein analysis with magnetic bead-based sampling capabilities. Lab on a Chip. 2002;2(1):27-30.
[6] Dittrich PS, Schwille P. An integrated microfluidic system for reaction, high-sensitivity detection, and sorting of fluorescent cells and particles. Analytical chemistry. 2003;75(21):5767-74.
[7] Munaz A, Shiddiky MJ, Nguyen N-T. Recent advances and current challenges in magnetophoresis based micro magnetofluidics. Biomicrofluidics. 2018;12(3).
[8] Jubery TZ, Srivastava SK, Dutta P. Dielectrophoretic separation of bioparticles in microdevices: A review. Electrophoresis. 2014;35(5):691-713.
[9] Connacher W, Zhang N, Huang A, Mei J, Zhang S, Gopesh T, Friend J. Micro/nano acoustofluidics: materials, phenomena, design, devices, and applications. Lab on a Chip. 2018;18(14):1952-96.
[10] Vigolo D, Rusconi R, Stone HA, Piazza R. Thermophoresis: microfluidics characterization and separation. Soft Matter. 2010;6(15):3489-93.
[11] Debnath N, Sadrzadeh M. Microfluidic mimic for colloid membrane filtration: a review. Journal of the Indian Institute of Science. 2018;98(2):137-57.
[12] Lenshof A, Laurell T. Continuous separation of cells and particles in microfluidic systems. Chemical Society Reviews. 2010;39(3):1203-17.
[13] Zhang J, Yan S, Yuan D, Alici G, Nguyen N-T, Warkiani ME, Li W. Fundamentals and applications of inertial microfluidics: A review. Lab on a Chip. 2016;16(1):10-34.
[14] Lu X, Liu C, Hu G, Xuan X. Particle manipulations in non-Newtonian microfluidics: A review. Journal of colloid and interface science. 2017;500:182-201.
[15] McGrath J, Jimenez M, Bridle H. Deterministic lateral displacement for particle separation: a review. Lab on a Chip. 2014;14(21):4139-58.
[16] Huang LR, Cox EC, Austin RH, Sturm JC. Continuous particle separation through deterministic lateral displacement. Science. 2004;304(5673):987-90.
[17] Inglis DW, Davis JA, Austin RH, Sturm JC. Critical particle size for fractionation by deterministic lateral displacement. Lab on a Chip. 2006;6(5):655-8.
[18] Davis JA. Microfluidic separation of blood components through deterministic lateral displacement: Princeton University; 2008.
[19] Beech JP. SEPARATION AND ANALYSIS OF BIOLOGICAL PARTICLES.
[20] Al-Fandi M, Al-Rousan M, Jaradat MA, Al-Ebbini L. New design for the separation of microorganisms using microfluidic deterministic lateral displacement. Robotics and computer-integrated manufacturing. 2011;27(2):237-44.
[21] Dincau BM, Aghilinejad A, Chen X, Moon SY, Kim J-H. Vortex-free high-Reynolds deterministic lateral displacement (DLD) via airfoil pillars. Microfluidics and Nanofluidics. 2018;22:1-9.
[22] Liu L, Loutherback K, Liao D, Yeater D, Lambert G, Estévez-Torres A, et al. A microfluidic device for continuous cancer cell culture and passage with hydrodynamic forces. Lab on a Chip. 2010;10(14):1807-13.
[23] Zeming KK, Ranjan S, Zhang Y. Rotational separation of non-spherical bioparticles using I-pillar arrays in a microfluidic device. Nature communications. 2013;4(1):1625.
[24] Hyun J-c, Hyun J, Wang S, Yang S. Improved pillar shape for deterministic lateral displacement separation method to maintain separation efficiency over a long period of time. Separation and Purification Technology. 2017;172:258-67
[25] Burlington MA. Multiphysics, C. O. M. S. O. L. Introduction to comsol multiphysics®. COMSOL Multiphysics, 1998. accessed Feb, 9(2018), 32.
[26] Bruus H. *Theoretical microfluidis* (Vol. 18): Oxford University Press; 2007
[27] Batchelor GK. *An introduction to fluid dynamics*: Cambridge University Press; 2000
[28] Beech J. Microfluidics separation and analysis of biological particles: Lund University; 2011.